Z-scan

de Dios P. [1] Nava A. [2]

[1−2]Laboratorio de Física Contemporánea II , Facultad de Ciencias, Universidad Nacional Autónoma de México,
Av. Universidad 3000, Circuito Exterior S/N, Delegación Coyoacán, C.P. 04510, Ciudad Universitaria, D.F. México.

Abstract

The Gaussian beam propagation method was employed to develop a computational code in Mathematica for simulating nonlinear optical effects in the Kerr medium using the Z-scan technique. The simulation results qualitatively reproduce the experimental behavior observed for ZIF particle samples, demonstrating the advantages of numerical studies for predicting nonlinear optical responses.

1. Introduction

Nonlinear optics studies the interaction between electromagnetic radiation and matter under conditions where the optical response of the medium is no longer proportional to the applied electric field, and consequently, the principle of superposition is no longer valid. This nonlinear behavior is generally described through the induced polarization P of the material in response to an electric field E.

The observation of nonlinear optical effects requires electromagnetic fields of very high intensity, comparable to interatomic electric fields (on the order of $10^8\,\mathrm{V/m}$). Such field strengths became experimentally accessible with the advent of laser sources. For this reason, the first experimental observations of nonlinear optical (NLO) phenomena coincided with the development of the first lasers. A notable example is the pioneering work of Peter Franken and collaborators in 1961 at the University of Michigan, who reported the first observation of second-harmonic generation. In their experiment, a green beam was generated from a quartz crystal illuminated by infrared radiation from a ruby laser.

In the regime of linear optics, the polarization induced in a material is directly proportional to the applied electric field and is given by

$$P = \epsilon_0 \chi^{(1)} E, \tag{1}$$

where ϵ_0 is the vacuum permittivity and $\chi^{(1)}$ is the linear electric susceptibility of the medium.

In contrast, when the applied electric field is sufficiently intense, the polarization response becomes nonlinear and can be expressed as a Taylor expansion in powers of the electric field:

$$P = \epsilon_0 \left(\chi^{(1)} E + \chi^{(2)} E^2 + \chi^{(3)} E^3 + \cdots \right), \tag{2}$$

or equivalently,

$$P = P^{(1)} + P^{(2)} + P^{(3)} + \cdots, \tag{3}$$

where $P^{(n)}$ denotes the n-th order contribution to the polarization. This expansion reflects the departure from a purely Hookean response of bound charges within the material.

For a dielectric medium interacting with an electromagnetic field, the electric displacement vector is defined as

$$\mathbf{D} = \epsilon_0 \mathbf{E} + \mathbf{P}. \tag{4}$$

If the medium is centrosymmetric, symmetry considerations dictate that the second-order susceptibility $\chi^{(2)}$ vanishes. Under this condition, the displacement vector reduces to

$$\mathbf{D} = \epsilon_0 \mathbf{E} + \epsilon_0 \chi^{(1)} \mathbf{E} + \epsilon_0 \chi^{(3)} \mathbf{E}^3. \tag{5}$$

Furthermore, many materials used in nonlinear optical experiments exhibit negligible magnetic response, such that their relative magnetic permeability is approximately unity ($\mu_r \approx 1$). Using the definition of the refractive index under these assumptions, it can be shown that the refractive index becomes intensity dependent and may be written as

$$n \approx n_0 + n_2 I, \tag{6}$$

where n_0 is the linear refractive index, I is the optical intensity, and

$$n_2 = \frac{3\chi^{(3)}}{4\epsilon_0 c n_0} \tag{7}$$

is the nonlinear refractive index. This intensity-dependent contribution to the refractive index gives rise to the optical Kerr effect, which is the main focus of this work.

1.1. Optical Kerr effect

The optical Kerr effect arises when an intense electromagnetic field induces a change in the dielectric properties of a material, resulting in a refractive index that depends on the optical intensity. This nonlinear response originates from the third-order electric susceptibility, $\chi^{(3)}$, and gives rise to both a nonlinear refractive index coefficient, n_2, and nonlinear absorption processes characterized by the coefficient β_0.

As a consequence of the Kerr nonlinearity, the propagating optical beam may undergo self-focusing or self-defocusing, depending on the sign of n_2. Specifically, a positive value of n_2 leads to an increase in the refractive in-

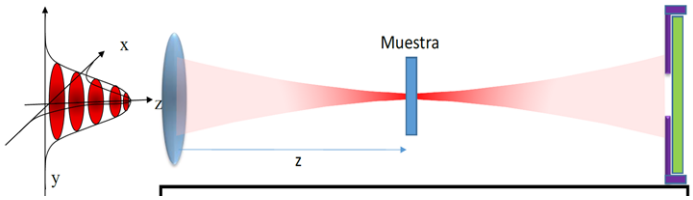

Figure 1: Schematic of the optical Kerr effect setup. A Kerr medium sample is placed in the midle of a Gaussian beam and a power meter.

dex with intensity, causing the beam to focus, whereas a negative value results in self-defocusing. Additionally, nonlinear absorption mechanisms, such as two-photon absorption, can lead to saturation effects within the material at sufficiently high intensities.

In a typical experimental configuration, once the linear absorption coefficient α_0 and the linear refractive index n_0 of the sample have been determined, the material is placed on a motorized translation stage near the focal region of a converging lens that focuses the laser beam. The sample is then translated along the optical axis (z-axis), and the transmitted optical signal passing through a finite aperture is measured as a function of the sample position. The resulting transmission profile contains information about the nonlinear refractive index and forms the basis of the Z-scan technique (see figure 2).

The experimental setup is commonly complemented by additional photodetectors that receive portions of the beam diverted by beam splitters. One detector is used to measure nonlinear absorption effects, while a second detector serves as a reference to compensate for fluctuations in the incident laser intensity. This differential detection scheme improves the accuracy and stability of the nonlinear optical measurements.

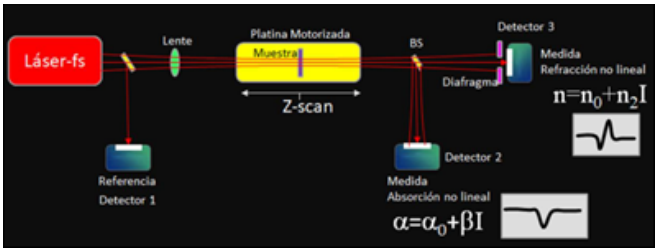

Figure 2: Z-Scan experimental arrangement.

1.2. Gaussian Beam Propagation and ABCD Matrix Formalism

The optical beams considered in this work are Gaussian beams, which constitute exact solutions of the paraxial wave equation. These beams are characterized by a transverse electric and magnetic field amplitude that follows a Gaussian spatial distribution. Gaussian beams play a central role in laser optics, as they accurately describe the output of many laser sources and allow for a compact analytical treatment of beam propagation through optical systems.

Under the paraxial approximation, the propagation of a Gaussian beam through an optical system can be efficiently described using the ray-transfer (ABCD) matrix formalism. In this framework, each optical element is represented by a 2×2 matrix that linearly relates the input and output ray parameters, such as the transverse position and propagation angle. This approach provides a powerful tool to track the evolution of key beam parameters, including the beam waist, wavefront curvature, and Gouy phase.

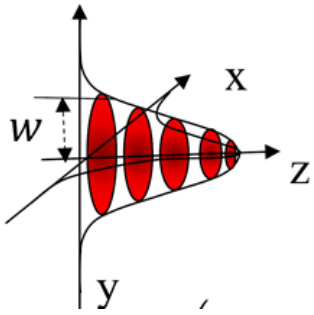

Figure 3: Transverse intensity profile of a Gaussian beam.

For a paraxial ray propagating in free space over a distance L, entering an optical element at transverse position r_1 with slope r_1', and exiting at position r_2 with slope r_2', the ray-transfer relation is given by

$$\begin{pmatrix} r_2 \\ r_2' \end{pmatrix} = \begin{pmatrix} 1 & L \\ 0 & 1 \end{pmatrix} \begin{pmatrix} r_1 \\ r_1' \end{pmatrix}. \tag{8}$$

In general, any optical element under the paraxial approximation can be represented by an ABCD matrix with elements A, B, C, and D. When a Gaussian beam propagates through a sequence of n optical elements, the total system matrix is obtained by multiplying the individual matrices in the order of propagation:

$$\begin{pmatrix} A_T & B_T \\ C_T & D_T \end{pmatrix} = \begin{pmatrix} A_n & B_n \\ C_n & D_n \end{pmatrix} \cdots \begin{pmatrix} A_2 & B_2 \\ C_2 & D_2 \end{pmatrix} \begin{pmatrix} A_1 & B_1 \\ C_1 & D_1 \end{pmatrix}. \tag{9}$$

The evolution of a Gaussian beam through such an optical system is conveniently described using the complex beam parameter q, which transforms according to

$$q_n = \frac{A_T q_1 + B_T}{C_T q_1 + D_T}. \tag{10}$$

The complex beam parameter is defined as

$$\frac{1}{q(z)} = \frac{1}{R(z)} - i\frac{\lambda}{\pi n \omega^2(z)}, \tag{11}$$

where $R(z)$ is the radius of curvature of the wavefront, $\omega(z)$ is the beam radius at position z, λ is the wavelength, and

n is the refractive index of the medium.

From the transformed beam parameter q_n, the physical beam quantities can be extracted as

$$R_n = \frac{1}{\mathrm{Re}\left(\frac{1}{q_n}\right)}, \tag{12}$$

and

$$\omega_n = \left[-\frac{\lambda}{\pi n \,\mathrm{Im}\left(\frac{1}{q_n}\right)}\right]^{1/2}. \tag{13}$$

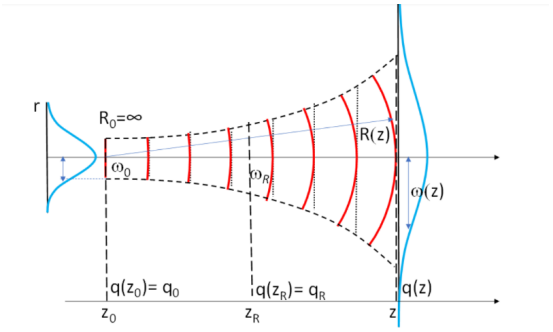

Figure 4: Beam waist and radius of curvature of a Gaussian beam.

To apply this formalism, the characteristic matrices of the optical elements involved must be specified. Common examples include:

$$\text{Free space: } \begin{pmatrix} 1 & L \\ 0 & 1 \end{pmatrix}$$

Transmission from a dielectric medium with refractive index n_1 to another with refractive index n_2:

$$\text{Dielectric interface: } \begin{pmatrix} 1 & 0 \\ 0 & \frac{n_1}{n_2} \end{pmatrix}$$

Propagation through a thin lens with focal length f:

$$\text{Thin lens: } \begin{pmatrix} 1 & 0 \\ -\frac{1}{f} & 1 \end{pmatrix}$$

Propagation through a gradient-index (GRIN) medium of thickness Δd, linear refractive index n_0, and effective nonlinear refractive index n_{GRIN} is described by

$$\text{GRIN lens: } \begin{pmatrix} 1 & \Delta d \\ -\frac{n_{\mathrm{GRIN}}}{n_0}\Delta d & 1 \end{pmatrix}. \tag{14}$$

In the presence of the optical Kerr effect, the nonlinear medium can be modeled as an intensity-dependent lens, commonly referred to as a Kerr lens. For a Kerr medium of thickness Δd, the corresponding ABCD matrix is

$$\text{Kerr lens: } \begin{pmatrix} 1 & \Delta d \\ -\frac{1}{h^2_{\mathrm{kerr}}(z)}\Delta d & 1 \end{pmatrix}, \tag{15}$$

where the Kerr parameter is defined as

$$\frac{1}{h^2_{\mathrm{kerr}}(z)} = \frac{8 n_2 P_L}{n_0 \pi \omega_L^4(z)} = \frac{n_{\mathrm{GRIN}}}{n_0}. \tag{16}$$

For the optical system considered in this work, the total Gaussian beam propagation is described by the matrix product

$$\begin{pmatrix} A_T & B_T \\ C_T & D_T \end{pmatrix} =$$

$$\begin{pmatrix} 1 & L_3 \\ 0 & 1 \end{pmatrix}\begin{pmatrix} 1 & 0 \\ 0 & \frac{n_0}{1} \end{pmatrix}\begin{pmatrix} 1 & \Delta d \\ -\frac{1}{h^2_{kerr(z)}}\Delta d & 1 \end{pmatrix}\begin{pmatrix} 1 & 0 \\ 0 & \frac{1}{n_0} \end{pmatrix}\cdot$$

$$\cdot\begin{pmatrix} 1 & L_2 \\ 0 & 1 \end{pmatrix}\begin{pmatrix} 1 & 0 \\ -\frac{1}{f} & 1 \end{pmatrix}\begin{pmatrix} 1 & L_1 \\ 0 & 1 \end{pmatrix} \tag{17}$$

2. Numerical Z-scan Simulation

In order to qualitatively reproduce the results obtained using the Z-scan technique, the Gaussian beam propagation formalism described in the previous section was implemented numerically using *Mathematica*. This software was selected due to its efficiency in performing symbolic and numerical matrix operations, as well as its robust handling of complex-valued quantities, which are essential for modeling Gaussian beam propagation through optical systems.

The simulations were carried out under the paraxial approximation, assuming a monochromatic, linearly polarized Gaussian beam. All physical parameters employed in the numerical model are defined below.

- $\omega_0 = 0.4$ mm: initial beam waist
- $d = 1$ mm: thickness of the Kerr medium
- $f = 0.13$ m: focal length of the converging lens
- $n_0 = 1.76$: linear refractive index of the Kerr medium
- $n_2 = 3 \times 10^{-3}$ m^2/W: nonlinear refractive index of the Kerr medium
- $\lambda = 800$ nm: laser wavelength
- $P = 100$ kW: laser power
- $l_1 = 0.13$ m: distance between the laser source and the lens
- $z_0 = -0.05$ m: initial position of the sample along the optical axis
- $z_f = 0.05$ m: final position of the sample along the optical axis
- $t = z_f - z_0$: total scan length
- $N = 200$: number of discrete steps in the Z-scan
- $h = \frac{t}{N}$: step size along the z-axis

- $q_0 = -i\frac{\pi n \omega_0^2}{\lambda}$: initial complex beam parameter
- $R = 0.5\,\omega_0$: radius of the diaphragm placed at the detector

The optical power transmitted through the diaphragm and collected by the detector is calculated by integrating the Gaussian intensity distribution over the aperture radius. This quantity is given by

$$g(\omega) = \int_{-R}^{R} I_0 \exp\left(-2\frac{r^2}{\omega^2}\right) dr, \tag{18}$$

where $I_0 = \frac{2P}{\pi\omega_0^2}$ is the peak intensity of the incident Gaussian beam. This expression allows the simulation of the detected signal as a function of beam width, which is essential for reproducing the characteristic Z-scan transmittance curves.

To validate the numerical implementation and gain insight into the behavior of the optical system, the simulation was initially applied to a simpler configuration consisting of a single converging lens, without including any nonlinear medium. In this preliminary case, the beam width was calculated as a function of the detector position around the focal plane using the ABCD matrix product given by Eq. (17), considering only the *free space–lens–free space* propagation sequence. The resulting data for *beam width* versus *detector position* are presented in Figure 5.

Subsequently, the full Z-scan configuration was implemented by introducing a nonlinear Kerr medium into the optical path. In this case, the medium was modeled as an intensity-dependent Kerr lens, and both the beam width and the transmitted power at the detector were computed as functions of the sample position along the optical axis. The Gaussian beam propagation was again described using the matrix formalism of Eq. (17). The simulated results for *beam width* versus *sample position* and *power* versus *sample position* are shown in Figures 6 and 7, respectively.

3. Results

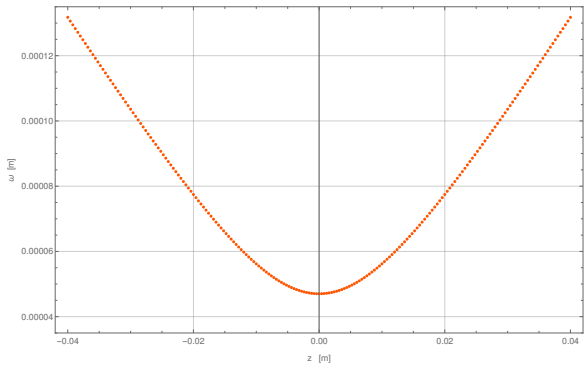

Figure 5: Detector position along the z-axis versus beam width ω using only a converging lens.

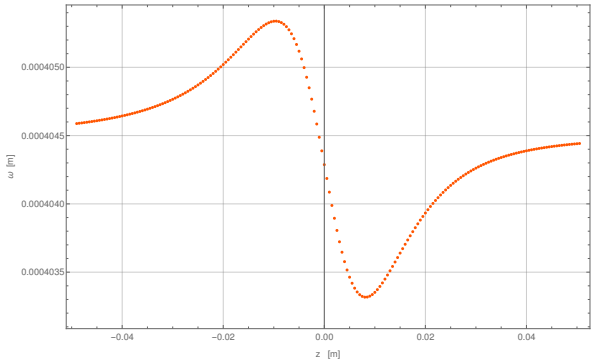

Figure 6: Position of the Kerr medium along the z-axis versus beam width ω.

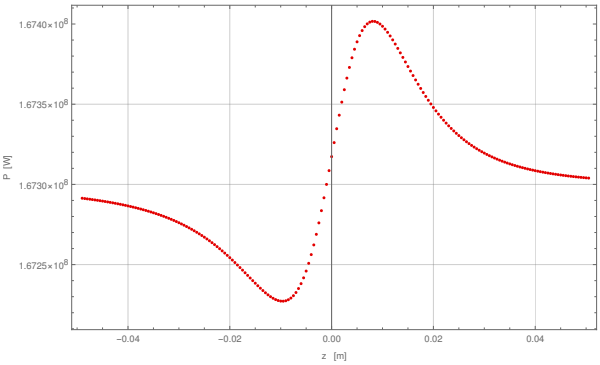

Figure 7: Position of the Kerr medium along the z-axis versus power measured at the detector.

The results corresponding to the converging lens configuration are presented in Figure 5, which shows the variation of the beam width as a function of the detector position along the optical axis. As expected, the beam reaches a minimum width near the focal plane of the lens and diverges symmetrically on either side, in agreement with Gaussian beam propagation theory.

Figure 6 presents the simulated beam width as a function of the sample position for the Z-scan configuration, where a nonlinear Kerr medium is introduced into the optical path. The presence of the nonlinear medium modifies the beam propagation due to the intensity-dependent refractive index, leading to variations in the beam width as the sample is translated through the focal region.

In addition, the corresponding variation of the optical power measured at the detector as a function of the sample position is shown in Figure 7. This transmittance curve reflects the combined effects of nonlinear refraction and the finite aperture at the detector, and constitutes a characteristic signature of the Z-scan technique.

4. Discussion

Figure 5 illustrates the dependence of the beam width on the detector position for the case of a single conver-

ging lens. The observed behavior is consistent with classical Gaussian beam optics: the beam waist increases as the detector is displaced away from the focal plane, while reaching a minimum value at the focal position. At this point, the beam width is comparable to the initial waist of the beam at the laser output, confirming the correct focusing behavior predicted by linear propagation theory.

Figure 6 shows the variation of the beam width when a nonlinear optical medium is introduced into the system. In this configuration, the Kerr medium exhibits an intensity-dependent refractive index, causing it to behave as an effective positive lens. As the sample is translated along the optical axis through the focal region, the nonlinear refraction leads to alternating self-focusing and self-defocusing of the beam, which manifests as a modulation of the beam width.

This nonlinear effect becomes more evident when a diaphragm is placed in front of the detector, as shown in Figure 7. In this case, the diaphragm radius is smaller than the initial beam width, making the detected signal highly sensitive to changes in beam size. Since the detected power is proportional to the spatially integrated beam intensity over the aperture, a wider beam results in lower collected power, whereas a narrower beam yields a higher detected power. Consequently, the power curve in Figure 7 exhibits a qualitative behavior that is the inverse of the beam-width variation shown in Figure 6, effectively appearing as a reflection with respect to the horizontal axis.

Finally, the qualitative trends observed in Figure 6 are in good agreement with experimental results reported in the literature and reproduced in laboratory measurements, such as those shown in Figure 8, where ZIF particles were employed as the nonlinear optical medium. In these experiments, the medium exhibits a response analogous to that of a converging lens, corroborating the validity of the Kerr lens model used in the numerical simulations.

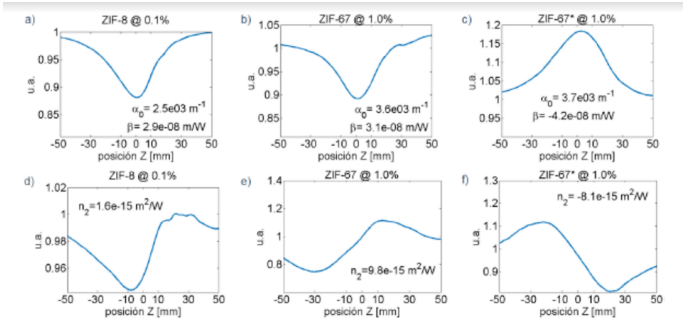

Figure 8: ZIF-8, appearance as a white powder (nanoparticles of 80 nm, dispersed in deionized water); ZIF-67, appearance as a purple powder (nanoparticles of 200 nm, dispersed in deionized water); and hydrolyzed ZIF-67 (aqueous dispersion with black color). a), b), c) Measurement with detector without diaphragm for the calculation of β; d), e), f) Measurement with detector with diaphragm, 20 % aperture, for the calculation of n_2.

5. Conclusions

The numerical simulations performed in this work successfully reproduce the qualitative behavior observed in the Z-scan technique, capturing the essential features associated with nonlinear refraction in Kerr media. In particular, the simulated beam-width modulation and transmitted power profiles are consistent with the characteristic signatures of self-focusing and self-defocusing effects.

Moreover, the Gaussian beam propagation method, combined with the ABCD matrix formalism, has been shown to provide a reliable and computationally efficient approximation for modeling nonlinear optical systems. This approach is especially useful when an a priori estimation of experimental outcomes is required, enabling the prediction of trends and qualitative responses before laboratory implementation.

Finally, the use of numerical simulations offers a significant advantage in terms of time and resource efficiency when compared to the execution of full experimental setups. By allowing rapid exploration of parameter spaces and anticipated system behavior, simulations serve as a valuable tool for optimizing experimental design and reducing trial-and-error efforts in the laboratory.

References

[1] Sainz, Arianeé. *Caracterización de propiedades ópticas no lineales por medio de la técnica de Z-Scan.* ICAT.

[2] Garduño, Jesus. *Metodo de propagacion de haces Gaussianos ABCD.*

[3] Hecht, Eugene. , *Optics*, Addison Wesley, 2000.

[4] Robert W. Boyd, *Nonlinear Optics*, Academic Press Inc., 1992

[5] Kogelnik H. *On the propagation of Gaussian Beams of Light Through Lens like Media Including those with a Loss or Gain Variation*, Applied Optics. 1562-1569 p 1965.

[6] Georgiev D., Herrmann, Stamm *Cavity design for optimum nonlinear absorption in Kerr-Lens modelocked.* 1992